MORPHOFUNCTIONAL EVALUATION IN DOME-SHAPED MACULA

A MICROPERIMETRY AND OPTICAL COHERENCE TOMOGRAPHY STUDY

ELISABETTA PILOTTO, MD, FEBO,* FRANCESCA GUIDOLIN, MD, FEBO,* MARIACRISTINA PARRAVANO, MD,† FRANCESCO VIOLA, MD,‡ DANIELE DE GERONIMO, MD,† ENRICA CONVENTO, MSc,* LAURA DELL'ARTI, MD,‡ ELENA TABACCHI, MSc,‡ RAFFAELE PARROZZANI, MD, PhD, FEBO,* FABIANO CAVARZERAN, ScD,* EDOARDO MIDENA, MD, PhD, FEBO, FARVO*†

Purpose: To investigate retinal sensitivity (Se) in dome-shaped macula (DSM) using microperimetry and to correlate functional findings to specific spectral domain optical coherence tomography features.

Methods: Patients affected by DSM in at least 1 eye were consecutively enrolled in a prospective, cross-sectional study. All studied eyes performed best-corrected visual acuity measurement, microperimetry to assess Se and optical coherence tomography to investigate DSM pattern and to measure bulge height and retinal and choroidal thicknesses.

Results: Fifty-three eyes of 29 patients were studied. Dome-shaped macula was vertically oriented (V-DSM) in 23 (43.4%), symmetric (S-DSM) in 17 (32.1%), and horizontally oriented (H-DSM) in 13 eyes (24.5%). Foveal subretinal fluid was present in 29/53 (54.7%) cases; it correlated to the bulge height ($P < 0.0001$) and determined a reduction of Se ($P < 0.0001$) not of best-corrected visual acuity ($P = 0.7105$). Mean Se was 13.9 ± 3.2 dB. Microperimetry parameters did not differ among the different DSM patterns. However, Se was significantly impaired if foveal subretinal fluid was present in V-DSM and in S-DSM, but not in H-DSM (V-DSM: $P < 0.0001$; S-DSM: $P = 0.0252$; H-DSM: $P = 0.5723$). In H-DSM, inferior choroidal thickness was thicker in cases with foveal subretinal fluid compared with those without it ($P = 0.0363$).

Conclusion: In DSM, Se evaluation better reflects the central functional impairment than best-corrected visual acuity, particularly when some optical coherence tomography features, such as foveal subretinal fluid and higher bulge height, are present.

RETINA 0:1–9, 2017

Dome-shaped macula (DSM) was first described by Gaucher et al[1] as a convex elevation of the macula within a myopic posterior staphyloma. Subsequently, it was also reported in myopic eyes without any staphyloma, in emmetropic, or in hypermetropic eyes.[2,3] Dome-shaped macula is best characterized by means of optical coherence tomography (OCT), particularly using enhanced depth imaging modality or swept source OCT, allowing for deeper tissue penetration into the choroid and the sclera.[2,4] Recently, Caillaux and associates described three morphologic DSM patterns according to spectral domain OCT (SD-OCT) features: round domes (without predominant axis), horizontally oriented oval-shaped domes, and vertically oriented oval-shaped domes.[5]

Potential vision-threatening macular complications, including choroidal neovascularization, retinal pigment epithelial changes, and subretinal fluid (SRF) without choroidal neovascularization, are well-established complications in DSM.[6,7] Although recent advances in OCT technology helped in evaluating DSM, its physiopathology remains uncertain. Various hypotheses have been proposed: scleral resistance to staphylomatous deformation, hypotony, alteration in vitreous traction vectors on the macula, localized choroidal thickening, and adaptive or compensatory

response to a myopic ocular expansion.[1,2,6,8] Moreover, a thicker choroid, localized on top of the inward bulge of the dome, has been proposed in the pathogenesis of the SRF, which is the main macular complication of DSM, occurring in almost one-third of the eyes, even without choroidal neovascularization.[7]

Even if DSM has been well described morphologically, its functional consequence has been poorly documented. The aim of the study was to investigate retinal function using microperimetry and to correlate retinal sensitivity (Se) to specific morphologic parameters identified with SD-OCT.

METHODS

Patients

Between March 1, 2015, and February 27, 2016, patients affected by DSM in at least one eye, attending the retinal unit of three Italian clinics, were consecutively enrolled in this prospective, cross-sectional study, according to a preplanned protocol. The 3 involved clinics were the Department of Ophthalmology of the University of Padova, the IRCCS-G. B. Bietti Foundation in Roma, and the Ophthalmological Unit, Ca' Granda Foundation-Ospedale Maggiore Policlinico of the University of Milano. All patients were visited in 1 retinal unit of every single center, and enrolled in the study. This study was conducted in accordance with the tenets of the Declaration of Helsinki and with the approval of each institutional ethical committee. After a detailed explanation of the purpose of this study, all enrolled patients signed a written consent form.

Exclusion criteria were signs of choroidal neovascularization, significant media opacity, uncontrolled intraocular pressure, and previous treatments involving macular area, i.e., photodynamic therapy and laser treatment.

The enrolled patients were evaluated with a complete ophthalmologic examination including best-corrected visual acuity (BCVA), using standard Early Treatment Diabetic Retinopathy Study (ETDRS) protocol, anterior segment examination; indirect ophthalmoscopy and 68-diopter-lens biomicroscopy, intraocular pressure, color fundus photography, SD-OCT, and microperimetry.

All examinations were performed during the same day (in the morning). All data obtained in the centers were collected in one of them and analyzed by three dedicated operators (E.P., F.G., E.C.).

Spectral Domain Optical Coherence Tomography: Imaging Acquisition and Analysis

Optical coherence tomography images were obtained using the Spectralis HRA+OCT system (Heidelberg Engineering, Heidelberg, Germany). The OCT protocol included two linear scans (6-mm horizontal and vertical scans centered on the fovea, in enhanced depth imaging modality, automated real time set at 100 frames) and a 30° × 25° posterior pole volume scan (centered onto the fovea, 120 μm apart, enhanced depth imaging modality, automated real time set at 50 frames). The caliber tool of the device was used for the following measurements: 1) subfoveal retinal thickness, defined as the distance between vitreoretinal interface and outer border of the photoreceptor layer (so that subfoveal fluid, eventually present, would not impair the estimation); 2) choroidal thickness (CT), defined as the distance between the outer border of the hyperreflective line, corresponding to the retinal pigment epithelium, and the inner scleral border, measured in five different points (subfoveally, 2 mm apart from the fovea, inferiorly, superiorly, nasally, and temporally); 3) macular bulge height (BH), defined as the distance between the outer border of the retinal pigment epithelium at the fovea and the line tangent to the outer border of retinal pigment epithelium on the borders of staphyloma, as described by Caillaux et al.[5] (Figure 1) The comparison between the BH in the horizontal versus the vertical scan allowed us to define the pattern of DSM.[5] All the 61 single linear horizontal scans of the. posterior pole volume scan were analyzed to detect the presence of SRF (subfoveally or extrafoveally), pigment epithelium detachment, subretinal climbs of macular pigment (SP), and macular schisis.

Microperimetry

Microperimetry was performed in mesopic condition using MP1 Microperimeter (Nidek, Gamagori, Japan). This technique has been previously described in detail.[9] For the purpose of this study, the following parameters were used: a red ring fixation target 1° in diameter; white, monochromatic background set at 1.27 cd/m^2 (=4 asb); stimulus size Goldmann III, with 200 milliseconds projection time; a 4-2 double staircase strategy; and a grid of 53 stimuli covering the

From the *Department of Ophthalmology, University of Padova, Padova, Italy; †G.B. Bietti Foundation, IRCCS, Roma, Italy; and ‡Ophthalmological Unit, Ca' Granda Foundation-Ospedale Maggiore Policlinico, University of Milano, Milan, Italy.

The research contribution by the G.B. Bietti Foundation was supported by Fondazione Roma and Ministry of Health.

None of the authors has any financial/conflicting interests to disclose.

F. Guidolin, M. Parravano and F. Viola have equally contributed to the study, and they present the same rights to its intellectual properties.

Reprint requests: Edoardo Midena, MD, PhD, FEBO, FARVO, via Giustiniani 2, 35100 Padova, Italy; e-mail: edoardo.midena@unipd.it

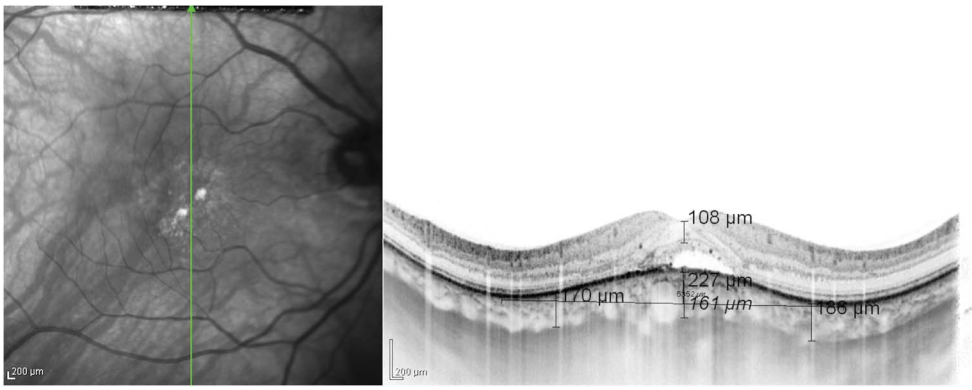

Fig. 1. Retinal, choroidal, and BH measurements at OCT horizontal linear scan in an eye with DSM.

central 20° (centered onto the fovea) (Figure 2). The following microperimetry parameters were than calculated: mean Se and mean residual Se. Dense scotoma was defined as tested loci that elicited no response even at the highest intensity stimulus (0 dB).[10]

Fixation stability was evaluated using data collected during a pure fixation task, asking the patient to fixate the target for 30 seconds (static fixation).[11] The fixation location was defined according to Fujii classification.[12] The quantification of fixation characteristics was performed using the bivariate contour ellipse calculated area (BCEA). The BCEA is an area which quantifies the horizontal and vertical eye positions and is expressed in degrees^2 (deg^2). This is a 2-dimensional ellipse that describes the portion of retinal surface within the center of the target imaged at least 68% of the time (BCEA 68), 95% of the time (BCEA 95), and 99% of the time (BCEA 99).[13]

Statistical Evaluation

Statistical analysis was conducted by SAS 9.3 on personal computer. Parameters were summarized according to the usual methods of descriptive statistics: mean, SD, median, and range (minimum, maximum) for quantitative continuous variables; frequency distribution, absolute and relative (percentage), for qualitative ones. The BH in the most cambered axis has been used for the statistical analysis. A comparison of CT among sectors was performed by means of analysis of covariance with repeated measures—some patients were evaluated on both eyes—and adjusted for spherical equivalent value of the eye. Correlation between Subfoveal SRF (*f*SRF) and DSM pattern was evaluated by means of logistic regression model. Correlations between microperimetry and OCT parameters (*f*SRF, pigment epithelium detachment, and SP) were evaluated by means of generalized linear model estimation (mixed effect models) adjusted for eye and spherical equivalent value. Repeated measures of parameters on both eyes of some patients were taken into consideration. Correlations between parameters and CT were also adjusted for eye and spherical equivalence value. Statistical tests were interpreted as significant if $P < 0.05$.

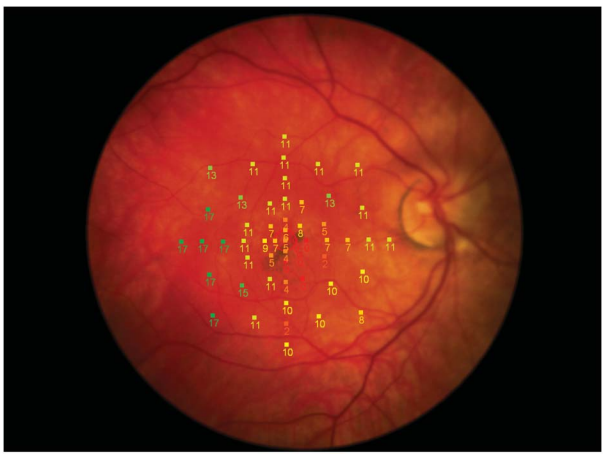

Fig. 2. Microperimetry sensitivity macular map in an eye with DSM.

RESULTS

Population Characteristics

Fifty-three eyes of 29 patients were consecutively evaluated. Dome-shaped macula was bilateral in 26 patients (89.66%). Sixteen patients were women (55.2%), and 13 were men (44.8%). Mean age was 57.4 ± 12.9 years (range 23–87). Mean spherical equivalent was −4.98 ± 4.77 D (range: from −16.25 to +1.75). Mean BCVA was 0.34 ± 0.36 logarithm of the minimum angle of resolution (range: from 1.0 to −0.2 logarithm of the minimum angle of resolution; 20/40 Snellen visual acuity; range from 20/200 to 20/12.5) (Table1).

Functional and Morphologic Parameters

Fixation was predominantly central in 41 eyes (77.36%), poorly central in 9 eyes (16.98%), and

Table 1. Demographic Data and OCT Parameters

Gender (Male/female), n (%)	13 (44.83%)/16 (55.17%)
Age (mean ± SD), years	57.4 ± 12.9
Spherical equivalent (mean ± SD), diopters	−4.98 ± 4.77
BCVA (Snellen) (mean, range)	20/40 (20/200–20/12.5)
Subfoveal retinal thickness (mean ± SD), μm	168.1 ± 49.1
CT (mean ± SD), μm	178.9 ± 101.9
Subfoveal	
2 mm superior	162.3 ± 87.6
2 mm inferior	154.6 ± 79.5
2 mm nasal	109.4 ± 70.2
2 mm temporal	153.9 ± 85.8
BH (in the most cambered axis) (mean ± SD), μm	168.1 ± 49.1
DSM pattern, n (%)	17 (32.08)
Symmetric	
Horizontally oriented	13 (24.53)
Vertically oriented	23 (43.40)
Presence of complications, n (%)	29 (54.72)
Foveal SRF	
Extrafoveal SRF	2 (3.77)
PED	18 (33.96)
Subretinal Pigment	26 (49.06)
Macular Schisis	2 (3.77)

PED, pigment epithelium detachment.

predominantly eccentric in 3 eyes (5.66%). Fixation was stable in 35 eyes (66.04%), relatively unstable in 15 eyes (28.30%), and unstable in 3 eyes (5.66%). Areas of fixation were 2.8 ± 3.2 deg^2 (BCEA 68), 7.6 ± 8.5 deg^2 (BCEA 95), and 13.5 ± 15.2 deg^2 (BCEA 99). Mean Se was 13.9 ± 3.2 dB, mean residual Se was 14.4 ± 2.8 dB, mean Se in the central 8° was 12.8 ± 4.3 dB, and mean Se in the central 4° was 11.3 ± 5.2 dB (Table 2).

Mean retinal thickness (calculated on horizontal and vertical scans) was 168.1 ± 49.1 μm (range 74–262 μm). Mean CT was 178.9 ± 101.9 μm subfoveally, 162.3 ± 87.6 μm 2 mm superiorly, 154.6 ± 79.5 μm 2 mm inferiorly, 109.4 ± 70.2 μm nasally, and 153.9 ± 85.8 μm temporally (Table 1). Choroid was thinner nasally than in all the other sectors (vs. subfoveal CT $P < 0.0001$; vs. superior CT, $P = 0.0001$; vs. inferior CT, $P < 0.0001$; vs. temporal CT, $P = 0.0002$). Mean BH was 494.4 ± 336 μm (range: from 71 to 1,359 μm) in the most cambered axis.

Subfoveal SRF was present in 29 eyes (54.72%) and extrafoveal SRF in 2 eyes (3.77%). Pigment epithelium detachment was detected in 18 eyes (33.96%), subretinal macular pigment climbs in 26 eyes (49.06%), and macular schisis in 2 eyes (3.77%).

Subfoveal SRF was correlated to the presence of SP but not to the presence of pigment epithelium detachment (Fisher exact test $P = 0.0023$ and $P = 0.2538$, respectively). Pigment epithelium detachment was not correlated to the presence of SP (Fisher exact test $P = 0.2542$).

In eyes with *f*SRF, BH was higher (625.5 ± 372.4 μm vs. 335.9 ± 196.5 μm, $P < 0.0001$) and Se was lower (Se: 12.9 ± 2.8 dB vs. 15.1 ± 3.2 dB, $P < 0.0001$; residual Se: 13.5 ± 2.5 dB vs. 15.5 ± 2.8 dB, $P < 0.0001$) than in eyes without it. Choroidal thickness was not different in any sectors between eyes with and without *f*SRF (Table 3).

In eyes with pigment epithelium detachment, Se was lower than in eyes without it, (Se: 12.5 ± 3.4 dB vs. 14.6 ± 2.9 dB, $P < 0.0360$; residual Se: 13.1 ± 3.1 dB vs. 15.1 ± 2.4 dB, $P < 0.0379$). The presence of SP did not reduce Se significantly (Se: 13.1 ± 2.8 dB vs. 14.7 ± 3.4 dB, $P = 0.8079$; residual Se: 13.5 ± 2.4 dB vs. 15.2 ± 2.9 dB, $P = 0.3742$).

Retinal sensitivity was correlated to subfoveal CT (Se: $P = 0.0463$; residual Se: $P = 0.0443$), to inferior CT (Se: $P = 0.007$; residual Se: $P = 0.0186$), to nasal CT (Se: $P = 0.0049$; residual Se: $P = 0.0139$), and temporal CT (Se: $P = 0.0393$; residual Se: $P = 0.0261$ for residual Se) (Table 4). Retinal sensitivity was correlated to BH (Se: $P = 0.007$; residual Se: $P = 0.0003$), even when corrected for the *f*SRF presence (Se: $P = 0.0405$; residual Se: $P = 0.0170$). Otherwise, BCVA was neither correlated to BH ($P = 0.6271$ and $P = 0.7576$ corrected for *f*SRF) nor to the presence of *f*SRF ($P = 0.6962$) (Table 5 and 6). Moreover, BCVA was neither correlated to PED ($P = 0.0725$) nor to the presence of SP ($P = 0.556$).

Table 2. Microperimetry Data

	Overall (n = 53)	V-DSM (n = 23)	H-DSM (n = 13)	S-DSM (n = 17)	*P**
Mean Se, dB	13.9 ± 3.2	14.0 ± 3.2	13.8 ± 2.6	13.9 ± 3.6	0.6899
Residual Se, dB	14.4 ± 2.8	14.4 ± 2.8	14.6 ± 2.2	14.3 ± 3.3	0.5375
BCEA 68, deg^2	2.8 ± 3.2	3.2 ± 3.9	2.5 ± 1.9	2.4 ± 2.9	0.7462
BCEA 95, deg^2	7.6 ± 8.5	8.8 ± 10.4	6.9 ± 5.1	6.4 ± 7.8	0.7403
BCEA 99, deg^2	13.5 ± 15.2	15.7 ± 18.6	12.3 ± 9.0	11.5 ± 14.0	0.7424

*One-way analysis of variance adjusted for repeated measures: eye.

dB, decibel; H-DSM, horizontally oriented dome-shaped macula; S-DSM, symmetric dome-shaped macula; V-DSM, vertically oriented dome-shaped macula.

Table 3. Influence of Foveal SRF on Morphologic and Functional Parameters

		Overall			V-DSM			H-DSM			S-DSM		
		*f*SRF			*f*SRF			*f*SRF			*f*SRF		
		No	Yes	*P*	No	Yes	*P*	No	Yes	*P*	No	Yes	*P*
	N	24	29		10	13		8	5		6	11	
BCVA, logMAR	Mean	0.34	0.35	0.7105*	0.38	0.36	0.6793	0.44	0.35	0.6962	0.14	0.33	0.3042
	SD	0.42	0.31		0.54	0.29		0.32	0.21		0.27	0.32	
Se, dB	Mean	15.1	12.9	**<0.0001***	16.6	11.9	**<0.0001**	13	15.2	0.5723	15.5	13	**0.0252**
	SD	3.2	2.8		2.0	2.4		2.1	3.1		4.6	2.8	
Residual Se, dB	Mean	15.5	13.5	**<0.0001***	16.7	12.6	**<0.0001**	13.8	16	0.2032	16.0	13.4	**0.0077**
	SD	2.8	2.5		2.0	1.8		1.7	2.3		4.0	2.6	
BH, μm	Mean	335.9	625.5	**<0.0001***	423.8	959.5	**0.0004**	290	322.8	0.1653	250.7	368.3	**0.0007**
	SD	196.5	372.4		244.8	283.3		143.1	62.2		116.6	163.6	
sfCT, μm	Mean	165.0	190.4	0.9021*	236.8	224.9	0.2031	103.3	113.2	0.7679	127.8	184.8	0.0659
	SD	115.5	89.7		141.1	101.7		38.2	56.3		73.5	65.3	
supCT, μm	Mean	155.2	168.2	0.9671*	215.3	183.1	0.4516	106.1	89.4	0.6962	120.3	186.5	0.3042
	SD	92.1	85.0		109.9	92.5		26.6	28.3		61.1	76.6	
infCT, μm	Mean	152.4	156.5	0.7674*	205.9	176.5	0.3725	97.4	139.6	**0.0363**	136.5	140.5	0.4406
	SD	89.1	72.2		105.0	82.9		46.6	97.8		52.8	39.8	
nasCT, μm	Mean	97.6	119.1	0.9769*	128.6	157.4	0.9410	63.6	73.4	0.5248	91.2	94.6	0.8456
	SD	69.2	70.8		89.2	83.6		41.9	42.5		37.5	36.3	
tempCT, μm	Mean	144.4	161.8	0.5279*	211.9	173.5	0.6793	83.3	148.0	0.1359	113.3	154.4	0.4431
	SD	111.4	57.0		136.1	67.6		46.5	37.9		66.6	51.9	

Significant *P*-value in bold.

*One-way analysis of variance, adjusted for spherical equivalent and repeated measures: eye.

dB, decibel; H-DSM, horizontally oriented dome-shaped macula; inf, inferior; logMAR, logarithm of the minimum angle of resolution; n.e., not estimabe; nas, nasal; SD, standard deviation; S-DSM, symmetric dome-shaped macula; sf, subfoveal; sup, superior; temp, temporal; V-DSM, vertically oriented dome-shaped macula.

Table 4. Correlation Between CT and Se

	Overall		V-DSM		H-DSM		S-DSM	
	Estimate	*P*	Estimate	*P*	Estimate	*P*	Estimate	*P*
Subfoveal CT								
Se	0.01033	**0.0463**	0.009176	0.2172	0.01478	0.3243	−0.01060	0.2458
Residual Se	0.00851	**0.0443**	0.007145	0.2304	0.01147	0.3586	−0.01995	**0.0058**
Superior CT								
Se	0.00659	0.1770	0.009955	0.1852	0.07272	**0.0011**	0.006367	0.5808
Residual Se	0.00512	0.1718	0.008112	0.1565	0.04215	**0.0209**	0.003276	0.7587
Inferior CT								
Se	0.01687	**0.0070**	0.01265	0.1808	0.005796	0.6537	0.04893	**0.0262**
Residual Se	0.01285	**0.0186**	0.007462	0.3635	0.004848	0.6584	0.04731	**0.0198**
Nasal CT								
Se	0.02096	**0.0049**	0.002444	0.8035	0.03038	**0.0243**	Did not converge	
Residual Se	0.01549	**0.0139**	−0.00039	0.9619	0.02427	**0.0302**	−0.03961	<**0.0001**
Temporal CT								
Se	0.01139	**0.0393**	0.008445	0.2834	0.03430	**0.0099**	0.02061	0.1020
Residual Se	0.00993	**0.0261**	0.006950	0.2742	0.01974	**0.0491**	0.01695	0.1590

Significant *P*-value in bold.
H-DSM, horizontally oriented dome-shaped macula; S-DSM, symmetric dome-shaped macula; V-DSM, vertically oriented dome-shaped macula.

Morphologic and Functional Parameters in the Different Dome-Shaped Macula Patterns

The DSM was vertically oriented (V-DSM) in 23 (43.4%), symmetric (S-DSM) in 17 (32.1%), and horizontally oriented (H-DSM) in 13 eyes (24.5%). In bilateral cases (26/29, 89.66%), the same type of dome was detected in 19/26 patients (73.08%); it was V-DSM in 9/19 (47.36%), H-DSM in 5/19 (26.32%), and S-DSM in 5/19 (26.32%). In the remaining cases (7/26 patients), the eyes had a different pattern.

Mean spherical equivalent was −4.71 ± 4.59 D in S-DSM, −6.33 ± 6.74 D in H-DSM, and −4.42 ± 3.50 D in V-DSM. There were no differences among DSM patterns regarding spherical equivalent (P = 0.9861), BCVA (P = 0.3380), fixation stability, and location (P = 0.4605 and P = 0.8291, respectively), fixation stability described as BCEA (P = 0.7462, P = 0.7401, and P = 0.7424 for 68.2, 95.4, and 99.6%, respectively), Se (both Se and residual Se, P = 0.6899 and P = 0.5375, respectively), and retinal thickness (P = 0.2971). Subfoveal SRF was present in 13/23 (56.5%) cases of V-SDM, in 5/13 (38.5%) cases of H-DSM, and in 9/13 (64.7%) cases of S-DSM.

Bulge height was significantly greater in V-DSM compared with both S-DSM (726.6 ± 376.9 μm vs. 326.8 ± 156.0 respectively, P = 0.0067) and H-DSM (726.6 ± 376.9 μm vs. 302.6 ± 116.2, P = 0.0011) (Figure 3). Among V-DSM and S-DSM cases, eyes with *f*SRF had a higher BH compared with those without it (Table 3). Subfoveal CT and superior CT were significantly thicker in V-DSM compared with H-DSM (230.0 ± 117.6 μm vs. 107.1 ± 44.0, P = 0.0218, and 197.1 ± 99.4 μm vs. 99.7 ± 27.4, P = 0.0356, respectively). The measurements performed at the OCT scans in the three different DSM patterns are summarized in Figure 3. Among the H-DSM cases, eyes with *f*SRF had a thicker choroid inferiorly compared with those without it (139.6 ± 97.8 μm vs. 97.4 ± 46.6 μm, P = 0.0363 (Table 3). The presence of *f*SRF did not significantly reduce BCVA in any of the DSM patterns (V-DSM: P = 0.7105; H-DSM: P = 0.6793; S-DSM: P = 0.3042). Conversely, Se was significantly impaired by the presence of *f*SRF

Table 5. Correlation Between BH and Se and BCVA by Type of Dome Shape

	Overall		V-DSM		H-DSM		S-DSM	
Parameter	Estimate	*P*	Estimate	*P*	Estimate	*P*	Estimate	*P*
Se	−0.00504	**0.0007**	−0.00681	**0.0006**	0.00027	0.9644	−0.01615	<**0.0001**
Residual Se	−0.00466	**0.0003**	−0.00365	**0.0251**	0.00194	0.6999	−0.01403	**0.0111**
BCVA	0.00008	0.6271	−0.00005	0.8403	−0.00062	**0.0008**	n.c.	

Estimation corrected for spherical equivalent.
Significant *P*-value in bold.
H-DSM, horizontally oriented dome-shaped macula; n.c., estimation algorithm did not converge; S-DSM, symmetric dome-shaped macula; V-DSM, vertically oriented dome-shaped macula.

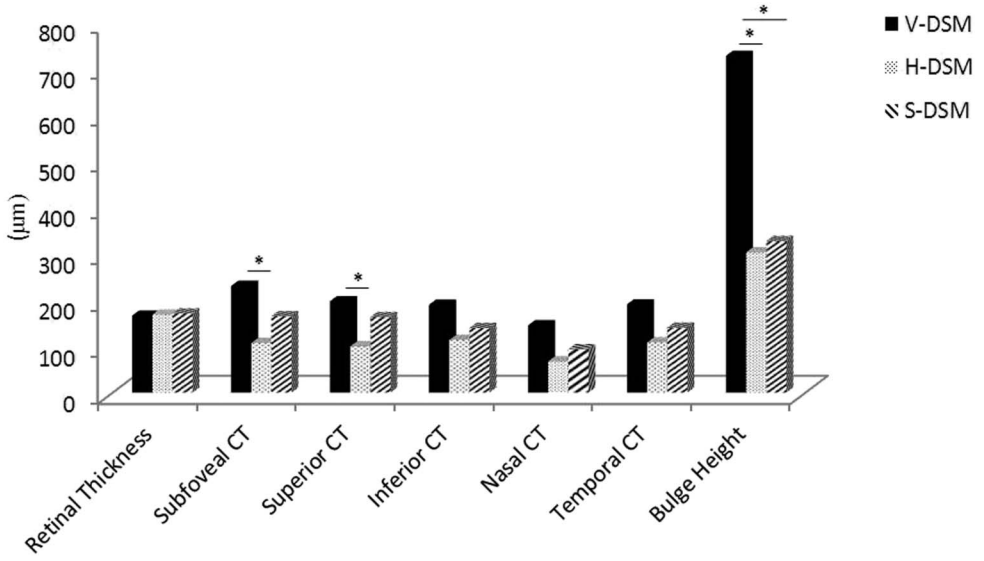

Fig. 3. Graph showing BH, retinal, and CT measurements in the three different patterns of DSM.

in the V-DSM and S-DSM patterns (both Se and residual Se: $P < 0.0001$ in V-DSM; Se: $P = 0.0252$, residual Se: $P = 0077$ in S-DSM) (Table 3). A significant correlation between Se and BH was still present when corrected for the presence of *f*SRF only in the S-DSM (Se: $P = 0.013$ residual Se: $P = 0.0111$) (Table 6).

Retinal sensitivity was correlated to subfoveal CT (Se: $P = 0.0463$; residual Se: $P = 0.0443$), to inferior CT (Se: $P = 0.007$; residual Se: $P = 0.0186$), to nasal CT (Se: $P = 0.0049$; residual Se: $P = 0.0139$), and to temporal CT (Se: $P = 0.0393$; residual Se: $P = 0.0261$ for residual Se) (Table 4).

DISCUSSION

Dome-shaped macula is an anomalous morphologic conformation of the macular area characterized by peculiar well-described SD-OCT features, usually occurring in myopic eyes, but also in eyes with mild myopia or emmetropia,[1–3,5,7,14,15] as confirmed by our study. However, except for visual acuity measurement, the functional impact has never been investigated in detail. In this study, we measured Se by means of microperimetry, detecting that it was reduced (13.9 ± 3.2 dB), more than reported in normal (17.9 ± 12 dB) or in highly myopic eyes (16.32 ± 2.6 dB).[16,17] Having used a different microperimeter device, Se reported in a series of myopic eyes by Zaben et al[18] is not comparable with our finding.

Retinal sensitivity was negatively correlated to the presence of *f*SRF. This is the most frequent complication that occurs in eyes with DSM, as confirmed by our findings, being present in more than 50% of our cases, for which, to date, there is no validated therapy. The influence of *f*SRF on visual acuity has been previously investigated, with controversial findings. Caillaux et al[5] reported visual acuity reduction associated with *f*SRF. However, visual acuity decrease was not observed in Viola's series.[7] Our findings confirm that visual acuity was not affected by *f*SRF, even if significantly reduced Se (from 15.1 ± 3.2–12.9 ± 2.8 dB). In this study, the functional impairment was analyzed in the different DSM patterns. They differed neither in BCVA nor in

Table 6. Correlation Between BH and Functional Parameters (Se and BCVA) According to DSM Pattern Corrected for Subfoveal SRF Presence

	Overall		V-DSM		H-DSM		S-DSM	
Parameter	Estimate	*P*	Estimate	*P*	Estimate	*P*	Estimate	*P*
Se	−0.00311	**0.0405**	0.00098	0.5747	−0.00193	0.7821	−0.01818	**0.0013**
Residual Se	−0.00324	**0.0170**	0.00075	0.6185	−0.00034	0.9527	−0.01291	**0.0111**
BCVA	0.00006	0.7576	−0.00004	0.9031	n.c.		n.c.	

Estimation corrected for spherical equivalent and presence of subfoveal SRF.
Significant *P*-value in bold.
H-DSM, horizontally oriented dome-shaped macula; n.c., estimation algorithm did not converge; S-DSM, symmetric dome-shaped macula; V-DSM, vertically oriented dome-shaped macula.

Se. However, Se was differently impaired according to specific OCT features. Retinal sensitivity was also negatively influenced by the height of the bulge, particularly in the V-DSM and in the S-DSM. However, in the V-DSM, even if the BH was higher than in the S-DSM, Se was more impaired by the presence of *f*SRF than by the BH, probably because of the high prevalence of *f*SRF. The H-DSM was the pattern with smaller BH (302.6 ± 116.2 μm) and lower incidence of *f*SRF (38.46%). This could be the reason why H-DSM was the only DSM pattern in which the presence of *f*SRF was not related to Se ($P = 0.5723$).

As reported by Caillaux et al,[5] we detected a high prevalence of *f*SRF in the V-DSM (56.5% of the cases). Moreover, in our series, *f*SRF was also frequently present in the S-DSM (64.7% of the cases). V-DSM and S-DSM patterns share a dome-shaped profile in the horizontal axis OCT scan, which is, on the contrary, normal in the H-DSM. This peculiar conformation of the posterior pole, particularly of the choroid, could explain the high prevalence of *f*SRF in these two DSM patterns. The H-DSM was the pattern with smaller BH (302.6 ± 116.2 μm) and lower incidence of *f*SRF (38.46%). This could be the reason why H-DSM was the only DSM pattern in which the presence of *f*SRF was not related to Se ($P = 0.5723$).

Choroidal thickness was always thicker in V-DSM compared with the other two DSM patterns in all the analyzed sectors. In particular, this difference was significant subfoveally and superiorly between V-DSM and H-DSM. Moreover, choroid was usually thicker subfoveally than in the other choroidal sectors as previously reported.[5] The role of choroid in the pathogenesis of DSM has been largely investigated. Chebil et al[19] detected that CT was increased in highly myopic eyes with DSM compared with highly myopic eyes without DSM. Choroid produces biochemical mediators that seem to influence scleral growth.[20] It has been hypothesized that a thick choroid can be responsible for the convexity of the macular profile.[1] Furthermore, the reported inhomogeneity in CT was advocated as the determinant of *f*SRF, with a mechanism similar to that described in central serous chorioretinopathy.[1,2,5,8,19,21] A correlation between CT and Se has been observed in highly myopic eyes.[18] As previously reported, in our study, choroid was thinner nasally in all DSM patterns.[6,15] We also detected that the nasal thinning of the choroid was related to a reduction of both mean Se and residual Se, particularly in the H-DSM pattern. In H-DSM, superior, nasal, and temporal CT were related to Se. Viola et al[7] reported that inferior choroid was thicker in eyes with *f*SRF than in those without it. We observed a thicker inferior choroid in eyes with *f*SRF only in H-DSM pattern, but we found no functional correspondence. Our findings suggest that, when the dome is higher, such as in V-DSM, BH and *f*SRF are the major contributors to retinal function impairment, whereas in less cambered DSM, such as in the H-DSM, the CT seems to be the most important parameter influencing Se.

In H-DSM, macular profile appears convex exactly in the vertical axis, and we could measure CT near the point of change of curvature of macular profile, in which modifications in CT are expected; otherwise, in V-DSM, macular bulge is more pronounced, and the point of change of curvature can be visualized only in a larger OCT scan. This could also explain the different results among DSM patterns. The V-DSM was the most frequent pattern we observed, accounting for 43.40% of all cases, followed by S-DSM (32.07%) and H- DSM (24.53%). In previous reports, the H-DSM appears as the most frequent pattern, followed by S-DSM and V-DSM (the latter being sometimes absent in some studies).[5,6,14] However, most of the studies included Asian (mainly Japanese) patients or highly myopic eyes. Our data can be compared with other studies on white patients, in which the proportion of V-DSM ranges from 16.7% to 23.1%.[5,7,14] However, this is the first study where a high prevalence of V-DSM has been described, and it should be taken into account when comparing different populations. According to the protocol of this study, two orthogonal (horizontally and vertically oriented) OCT linear scans had to be acquired, as DSM pattern can not be adequately recognized if OCT scans are registered only in one direction. This can explain the different proportion of DSM patterns we observed.

This study has some limitations. First, the scleral thickness, whose role in the DSM formation has been hypothesized, was not investigated because, even if we used an SD-OCT in enhanced depth imaging modality, the outer scleral border is difficult to be visualized. Second, the small sample size; however, DSM is a relatively rare entity, newly described, whose prevalence, of about 10%, is mainly known among myopic eyes. Third, the duration of eventually present symptoms, and *f*SRF was not investigated. Acute *f*SRF could compromise Se and visual acuity differently compared with chronic *f*SRF. Finally, all measurements of choroidal and retinal thicknesses and the BH were carried out manually using a built-in caliper of the SD-OCT device; novel choroidal segmentation software may help future studies about this disease.

The main strength of this study is that the functional counterpart of some specific and well-described OCT features have been largely investigated using microperimetry. A follow-up microperimetry study could be useful to better evaluate the progression of visual function deterioration, particularly when long-standing *f*SRF occurs.

In conclusion, even if visual acuity may be not affected, retinal function may be compromised in DSM, particularly when some morphologic macular features are present. Therefore, an integrated morphologic and functional assessment is worthwhile in the evaluation of such a peculiar entity, and more effort should be done to adequately treat *f*SRF, being one of the most morphologic parameters that compromise Se.

Key words: dome-shaped macula, optical coherence tomography, microperimetry, retinal sensitivity.

References

1. Gaucher D, Erginay A, Lecleire-Collet A, et al. Dome-shaped macula in eyes with myopic posterior staphyloma. Am J Ophthalmol 2008;145:909–914.
2. Imamura Y, Iida T, Maruko I, et al. Enhanced depth imaging optical coherence tomography of the sclera in dome-shaped macula. Am J Ophthalmol 2011;151:297–302.
3. Errera M, Michaelides M, Keane PA, et al. The extended clinical phenotype of dome-shaped macula. Graefes Arch Clin Exp Ophthalmol 2014;252:499–508.
4. Ellabban AA, Tsujikawa A, Matsumoto A, et al. Three-dimensional tomographic features of dome-shaped macula by swept-source optical coherence tomography. Am J Ophthalmol 2013; 155:320–328.
5. Caillaux V, Gaucher D, Gualino V, et al. Morphologic characterization of dome-shaped macula in myopic eyes with serous macular detachment. Am J Ophthalmol 2013;156: 958–967.
6. Ohsugi H, Ikuno Y, Oshima K, et al. Morphologic characteristics of macular complications of a dome-shaped macula determined by swept-source optical coherence tomography. Am J Ophthalmol 2014;158:162–170.
7. Viola F, Dell'Arti L, Benatti E, et al. Choroidal findings in dome-shaped macula in highly myopic eyes: a Longitudinal Study. Am J Ophthalmol 2015;159:44–52.
8. Mehdizadeh M, Nowroozzadeh MH. Dome-shaped macula in eyes with myopic posterior staphyloma. Am J Ophthalmol 2008;146:478; author reply 478–479. [Comment on Dome-shaped macula in eyes with myopic posterior staphyloma. Am J Ophthalmol. 2008].
9. Midena E, Vujosevic S, Convento E, et al. Microperimetry and fundus autofluorescence in patients with early age-related macular degeneration. Br J Ophthalmol 2007;91:1499–1503.
10. Pilotto E, Guidolin F, Convento E, et al. Fundus autofluorescence and microperimetry in progressing geographic atrophy secondary to age-related macular degeneration. Br J Ophthalmol 2013;97:622–626.
11. Longhin E, Convento E, Pilotto E, et al. Static and dynamic retinal fixation stability in microperimetry. Can J Ophthalmol 2013;48:375–380.
12. Fujii GY, De Juan E Jr, Humayun MS, et al. Characteristics of visual loss by scanning laser ophthalmoscope microperimetry in eyes with subfoveal choroidal neovascularization secondary to age related macular degeneration. Am J Ophthalmol 2003; 136:1067–1078.
13. Bellmann C, Feely M, Crossland MD, et al. Fixation stability using central and pericentral fixation targets in patients with age-related macular degeneration. Ophthalmology 2004;111: 2265–2270.
14. Soudier G, Gaudric A, Gualino V, et al. Long-term evolution of dome-shaped macula: increased macular bulge is associated with extended macular atrophy. Retina 2016;36:944–952.
15. Ellabban AA, Tsujikawa A, Muraoka Y, et al. Dome-shaped macular configuration: longitudinal changes in the sclera and choroid by swept-source optical coherence tomography over two years. Am J Ophthalmol 2014;158:1062–1070.
16. Sabates FN, Vincent RD, Koulen P, et al. Normative data set identifying properties of the macula across age groups: integration of visual function and retinal structure with microperimetry and spectral-domain optical coherence tomography. Retina 2011;31:1294–1302.
17. Parravano M, Oddone F, Giorno P, et al. Influence of macular choroidal thickness on visual function in highly myopic eyes. Ophthalmic Res 2014;52:97–101.
18. Zaben A, Zapata MÁ, Garcia-Arumi J. Retinal sensitivity and choroidal thickness in high myopia. Retina 2015;35:398–406.
19. Chebil A, Ben Achour B, Chaker N, et al. Choroidal thickness assessment with SD-OCT in high myopia with dome-shaped macula. J Fr Ophtalmol 2014;37:37–41.
20. Nickla DL, Wallman J. The multifunctional choroid. Prog Retin Eye Res 2010;3:144–168.
21. Deobhakta A, Ross AH, Helal J Jr, et al. Localized choroidal thickness variation and pigment epithelial detachment in dome-shaped macula with subretinal fluid. Ophthalmic Surg Lasers Imaging Retina 2015;46:391–392.